

# Investigation of the heating characteristics of electron Bernstein wave via slow X-B mode conversion in LHD

Ryoma Yanai<sup>1)</sup>, Hiroe Igami<sup>1)</sup>, Masaki Nishiura<sup>1)</sup>  
 1) National Institute for Fusion Science



## Introduction

- The electron Bernstein wave (EBW) is an electrostatic mode wave in plasma. It can be a powerful auxiliary heating method because it has no density limit on its propagation.
- A mode conversion process such as X-B or O-X-B mode conversion is needed in plasmas to generate EBW. During the X-B mode conversion process in the upper hybrid resonance (UHR), parametric decay instability (PDI) occurs, through which a pump wave generates different frequency waves ( $f_0 = f_1 \pm f_2$ ).
- Some attempts of EBW heating have been conducted in LHD. In 23rd experimental campaign, a new ECH antenna of 77 GHz was installed to inject ECH perpendicularly to the magnetic field. This new antenna can be also used for EBW heating by direct X-B mode conversion.

## Experimental setup

- The LHD is a heliotron type device with a pair of  $l/m = 2/10$  helical coils. The LHD has 10-fold rotational symmetry.
- New metal mirrors for 77 GHz ECH were installed in the LHD since the 23rd experimental campaign and they were used for EBW heating in this experiment.
- A dipole antenna and a CTS measurement system were used to measure waves excited through PDI.
- The dipole antenna and the CTS receiver can measure relatively low RF emission and ECE, respectively.
- $(R_{ax}, B_t) = (3.9 \text{ m}, 2.63 \text{ T})$ ,  $\bar{n}_e < 1 \times 10^{19} \text{ m}^{-3}$ ,  $T_e \sim 3 - 4 \text{ keV}$ .

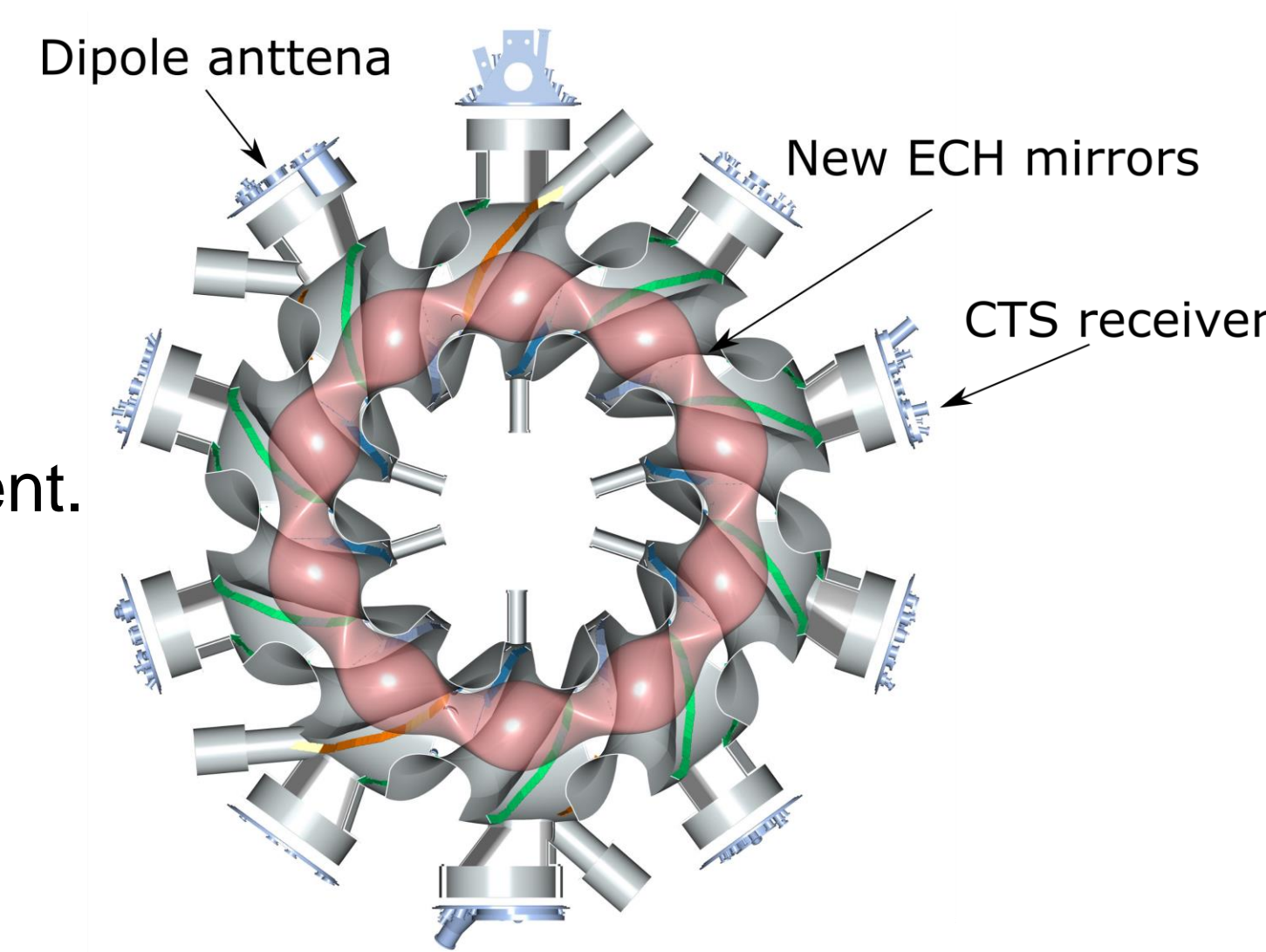


Figure 1. Schematic view of the LHD.

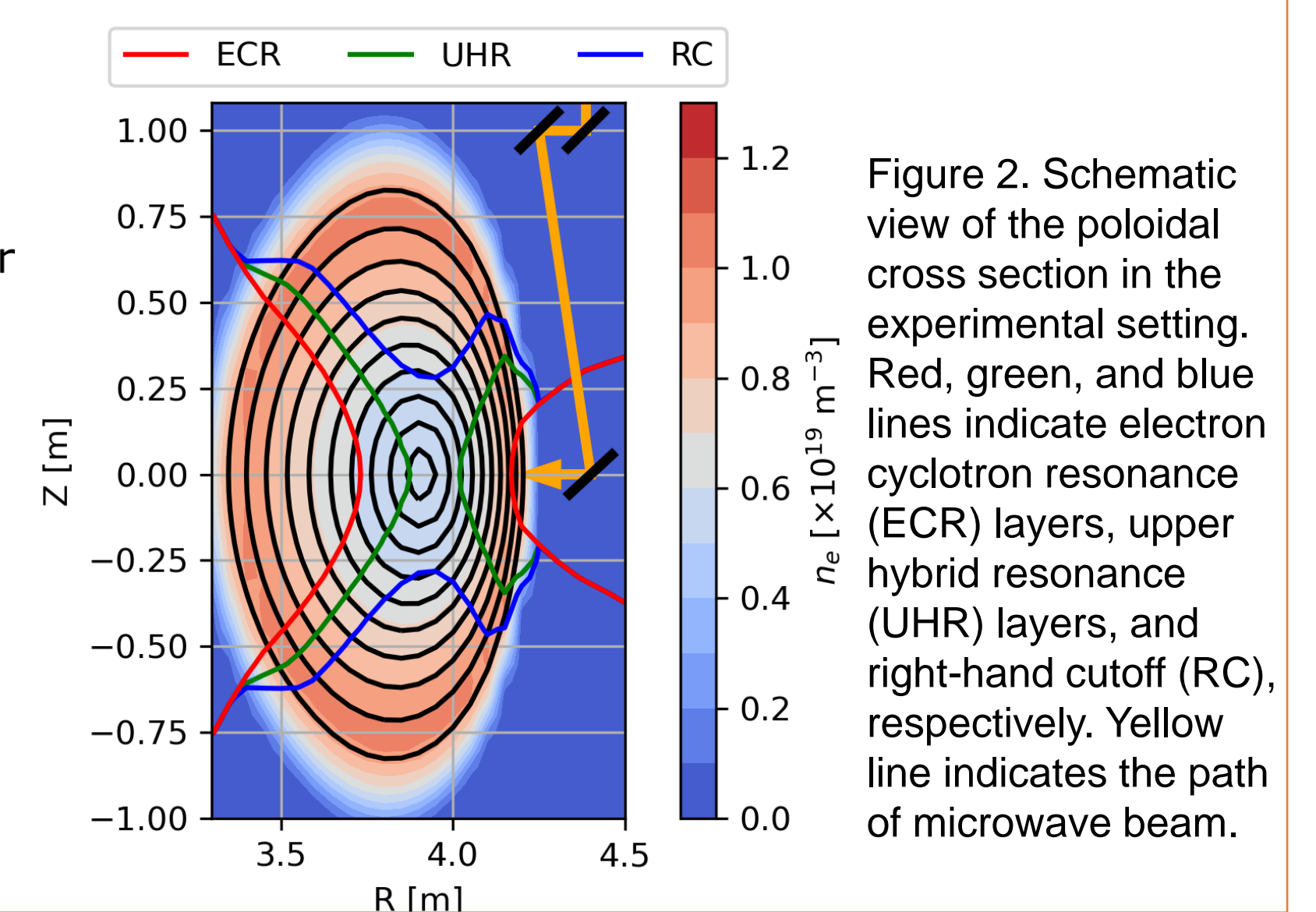


Figure 2. Schematic view of the poloidal cross section in the experimental setting. Red, green, and blue lines indicate electron cyclotron resonance (ECR) layers, upper hybrid resonance (UHR) layers, and right-hand cutoff (RC), respectively. Yellow line indicates the path of microwave beam.

## Results

### 1. Comparison of steady power injection by X-mode and O-mode waves

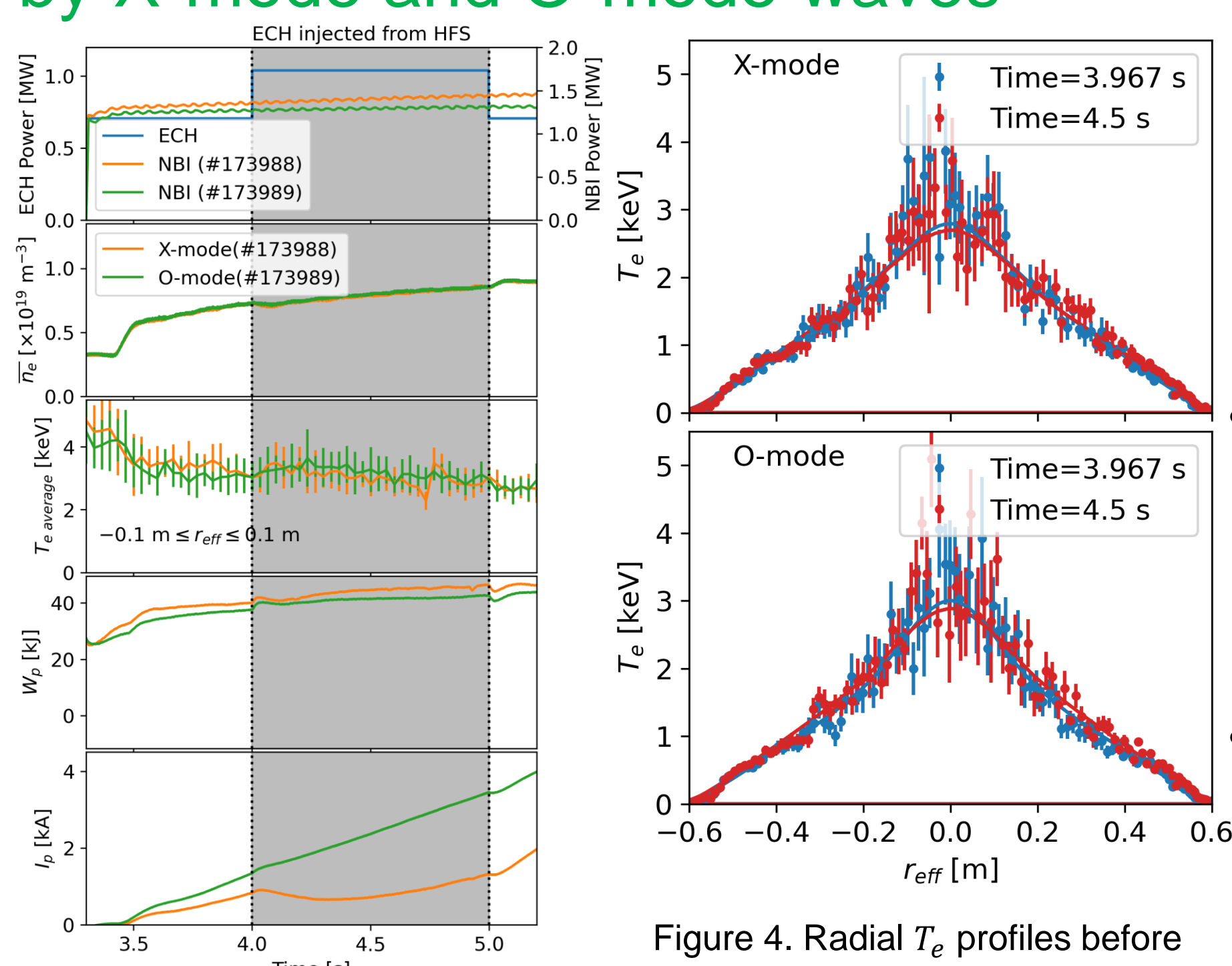


Figure 3. Time evolution of injection power of ECH and NBI,  $\bar{n}_e$ ,  $T_e$ ,  $W_p$  and  $I_p$ .

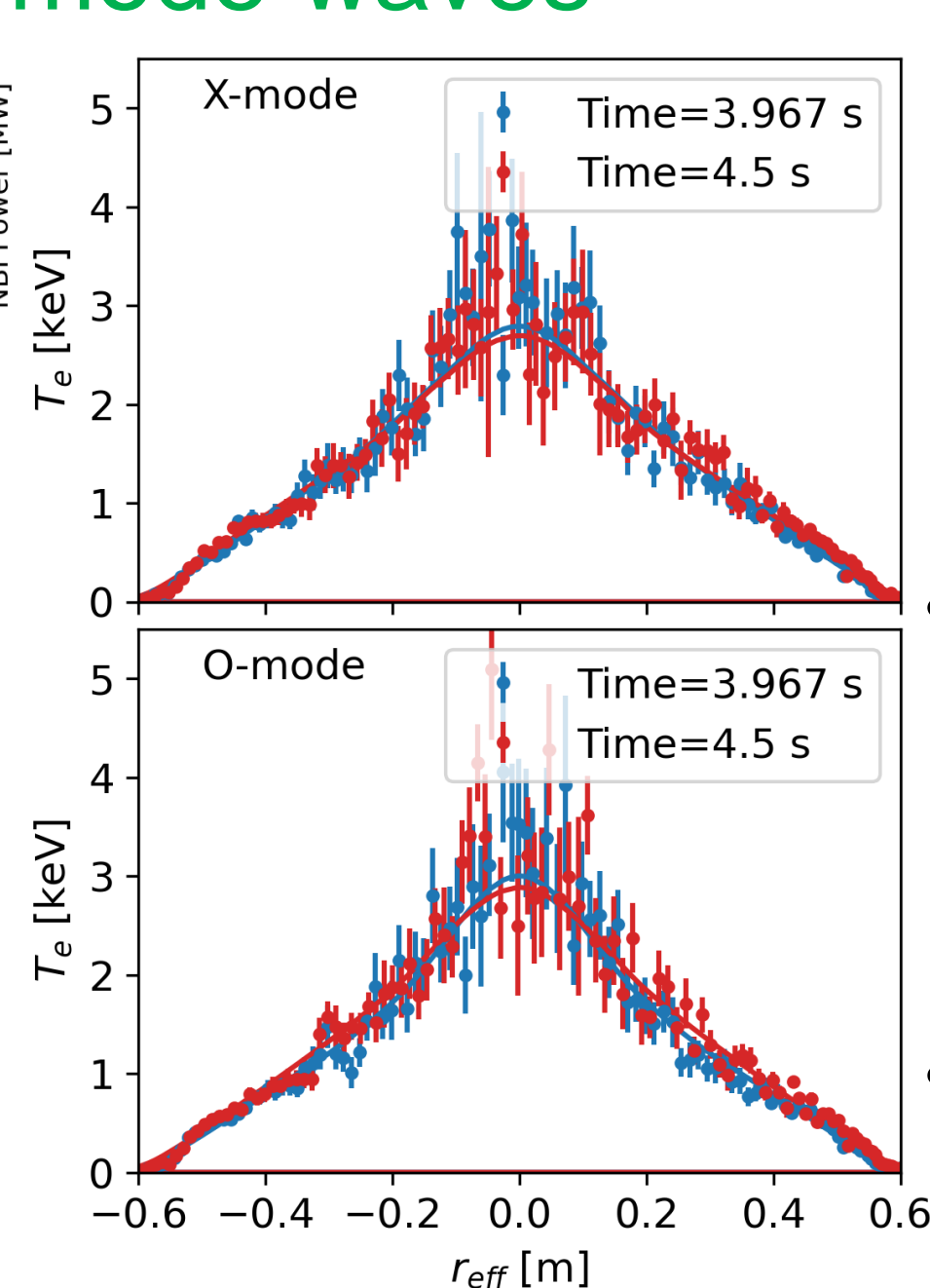


Figure 4. Radial  $T_e$  profiles before and during ECH injection

- Clear differences in  $T_e$  and  $W_p$  were not observed because the injected power was relatively low ( $\sim 300 \text{ kW}$ ) and ECR layer existed in the off-axis region.
- Plasma current driven by the X-mode wave injection was much larger than that of the O-mode wave injection.
- This difference implies that the X-mode wave was converted to the EBW which can drive large current because  $N_{||}$  of the excited EBW can be large.

### 2. Observation of waves excited through PDI

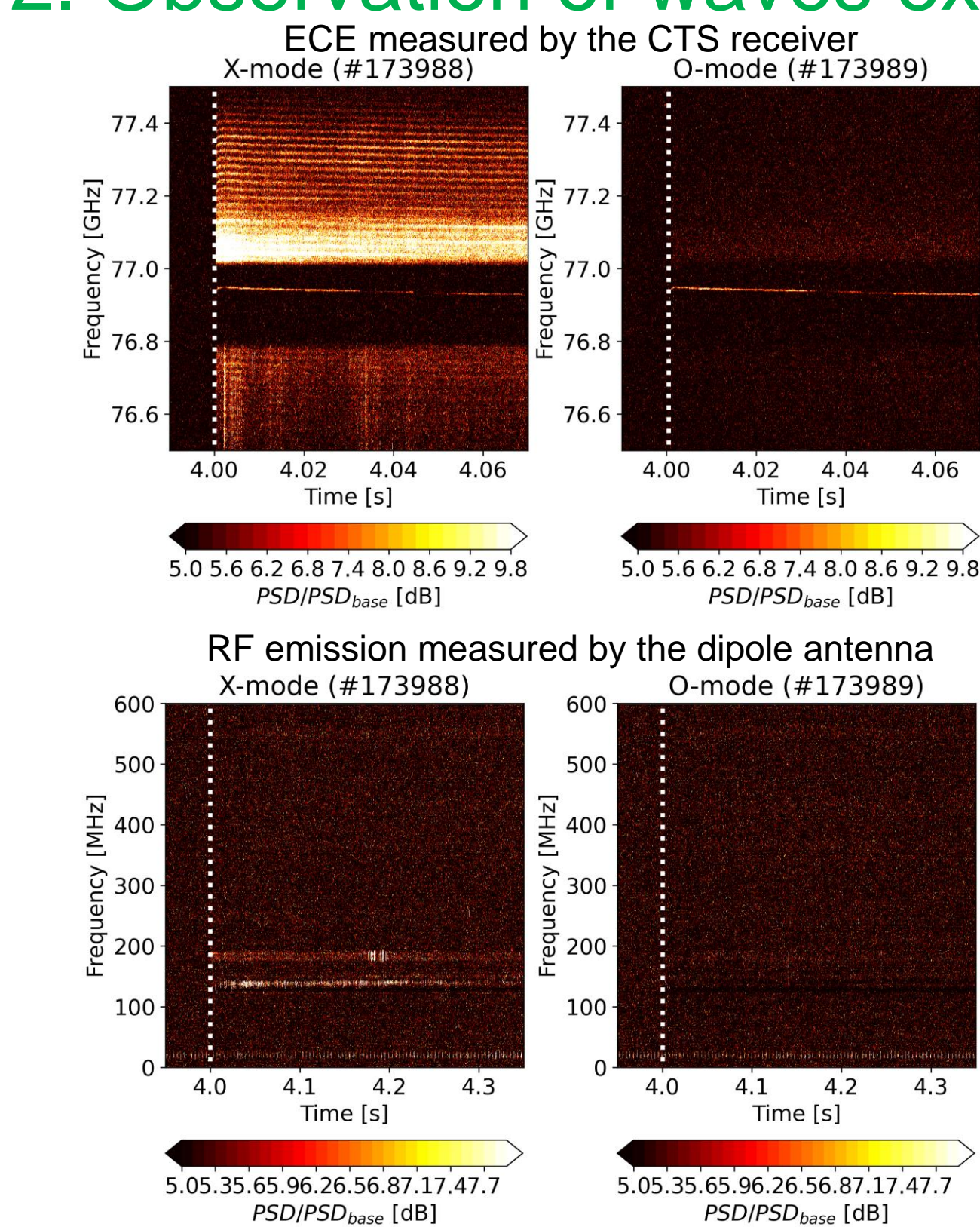


Figure 5. Spectrogram normalized by PSD before ECH injection (PSD<sub>base</sub>) of (top) ECE and (bottom) RF emission. White dotted lines shows the start of ECH injection.

- The radiation measured by dipole antenna and CTS receiver during the X-mode wave injection increased. These radiation increases may be caused by PDI.
- The ECE signal had significant power in wide frequency range while the power spectrum density (PSD) of the RF signal partly increased due to the frequency characteristic of the dipole antenna.
- It was difficult to confirm if the observed signals fulfilled  $f_0 = f_1 \pm f_2$ .

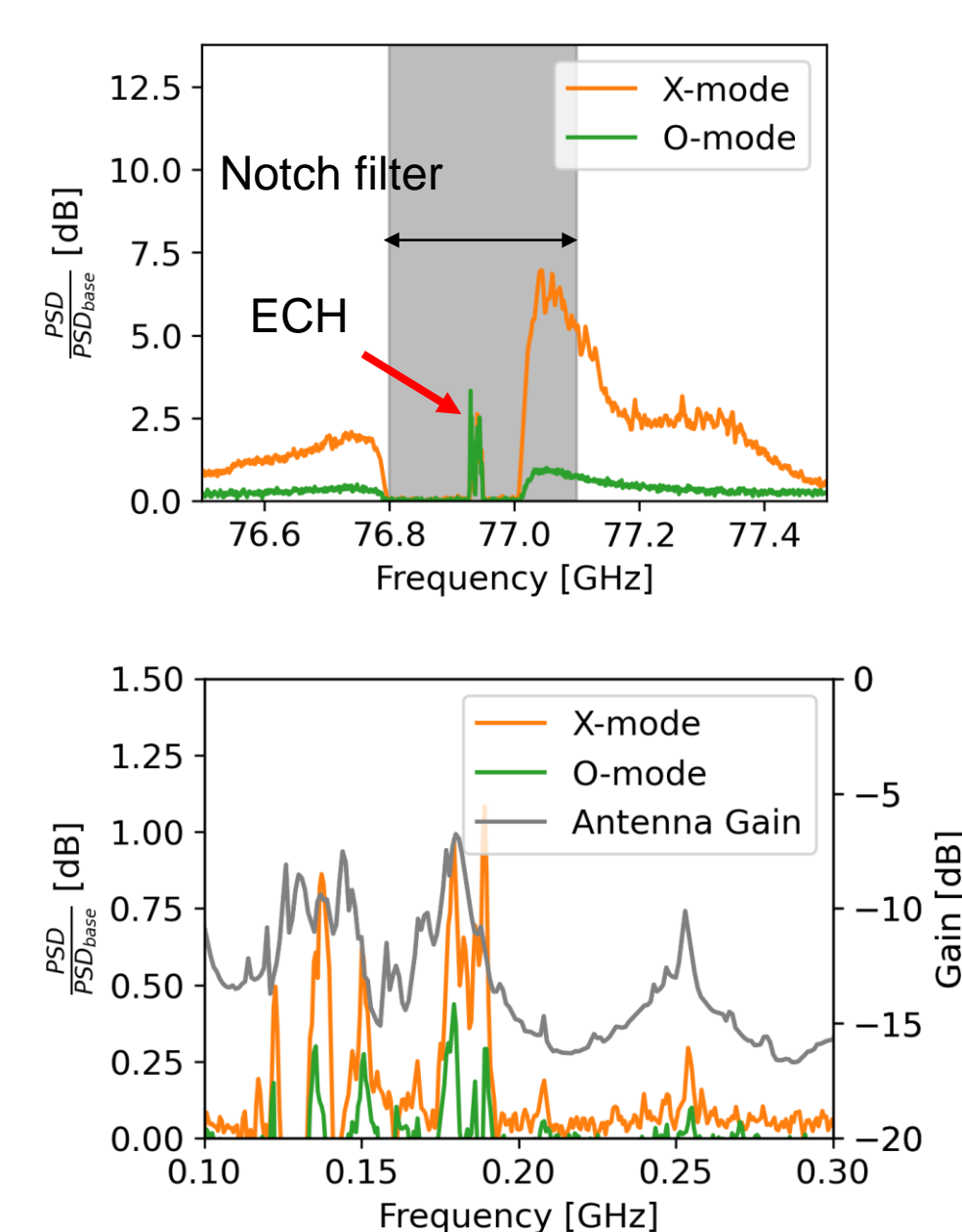


Figure 6. PSD of (top) ECE and (bottom) RF emission. Orange and green lines indicate the X-mode and O-mode injection cases, respectively. Gray line shows the dipole antenna gain.

### 3. Power absorption by power modulation experiment

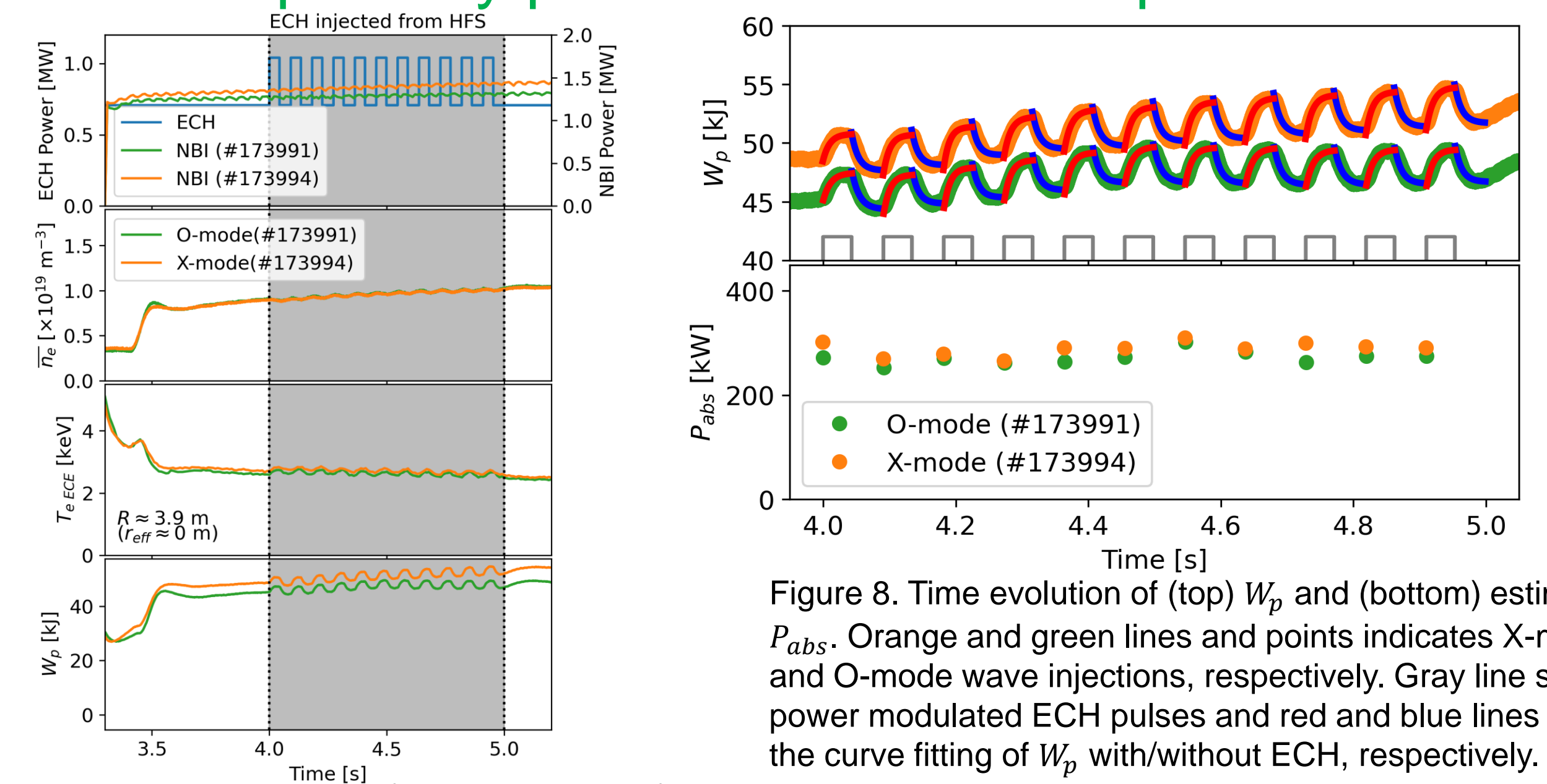


Figure 7. Time evolution of injection power of ECH and NBI,  $\bar{n}_e$ ,  $T_e$ ,  $W_p$ .

- The absorbed power ( $P_{abs}$ ) of X-mode and O-mode wave injections were estimated by modulating ECH power at 11 Hz.
- $P_{abs}$  was derived by applying the fitting function ( $W_p = P\tau_E + (W_{p0} - P\tau_E)e^{-t/\tau_E}$ ) and subtracting  $P$  with/without ECH in each modulation cycle ( $P_{abs} = P_{with\ ECH} - P_{without\ ECH}$ ).
- $P_{abs}$  was the almost same in both wave injections.

### 4. Comparison of the power deposition location

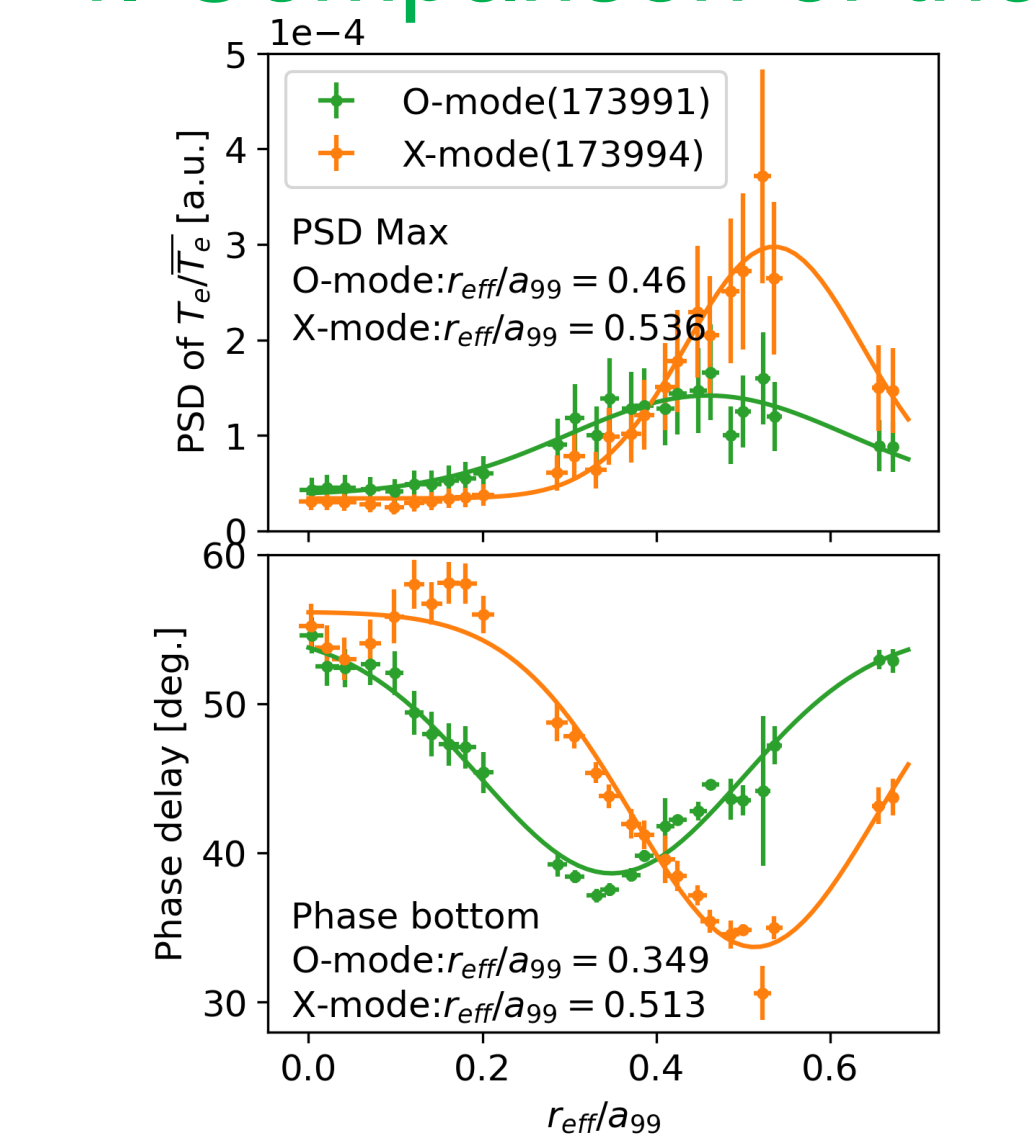


Figure 9. Radial profiles of the modulation frequency component of PSD and PD.

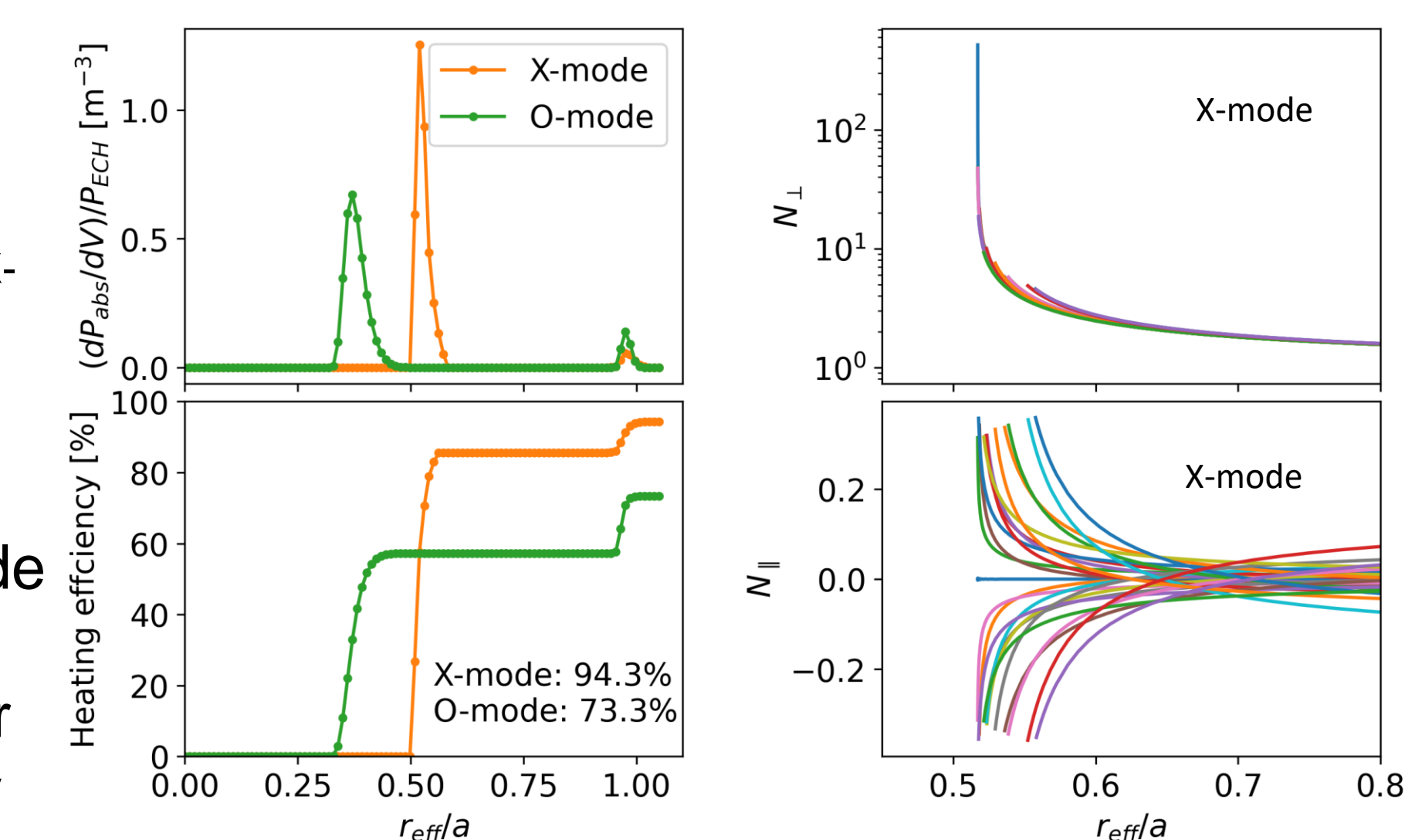


Figure 10. Radial profiles of the power deposition and the cumulative power of ECH calculated by TRAVIS.

- The power deposition locations were estimated by an FFT analysis of ECE and fitting radial profiles of PSD and the phase delay (PD) to the following functions to derive the center positions:
 
$$PSD = a^2 \exp(-(r_{eff}/a_{99} - b)^2/c^2) + d,$$

$$PD = a^2 \{1 - \exp(-(r_{eff}/a_{99} - b)^2/c^2)\} + d$$
- The power was absorbed around the UHR layer in the case of the X-mode wave and the O-mode wave was mainly absorbed in the inboard-side ECR layer.

- The power deposition locations calculated by TRAVIS were almost the same as the experimental results of both the X-mode and the O-mode wave injection although the wave propagation was calculated by using the cold plasma dispersion and  $N_{\perp}$  became too large.
- Therefore, the power may be absorbed to some extent during the mode conversion process in the X-mode injection case.

## Summary

- EBW heating via X-B mode conversion using a new ECH antenna system was demonstrated in the limited condition (setting low density and the magnetic axis outward).
- Clear differences of the X-mode and O-mode wave injection in plasma current, RF emission and ECE which may originate from PDI were observed.
- Absorbed power estimated from  $W_p$  was the almost same in both the X-mode and O-mode wave injection.
- The power deposition position of the X-mode wave injection was farther from the magnetic axis than that of the O-mode wave injection because the O-mode wave was absorbed in the inboard-side ECR layer while the excited EBW was absorbed around UHR layer due to the Doppler effect.
- The power can be absorbed during the X-B mode conversion in the X-mode wave injection case.